Long-wave Instability in Double-diffusive Marangoni Convection

Jean-Luc Thiffeault

1 Introduction

In fluid convection with a free surface at the top it is sometimes the case that surface tension effects become important. For instance in conditions of microgravity (e.g. crystal growth in a space shuttle when a free surface is present) the gravitational forces are negligible [1, 2]; Or, as in Bénard's original experiments, the layer of fluid is very thin and the convection is surface-tension dominated [3, 4]. We consider here the case of two diffusing quantities (for convenience referred to as heat and salt) with those surface tension effects taken into account. We shall be particularly interested in the diffusive regime where overstability occurs. We will derive a small amplitude long-wave planform equation for the case where fixed fluxes of heat and salt are imposed at the top and bottom boundaries, and find a long-wave equation capturing the low-order bifurcation structure of a co-dimension two Takens–Bogdanov point. We discuss the possibility of capturing a larger portion of the bifurcation by adding surface deformation effects to tune out resonant nonlinear terms.

2 Governing Equations of the System

The equations describing the temporal evolution of the system are the usual ones for two-dimensional thermohaline convection in the Boussinesq approximation:

$$\begin{aligned}
\frac{1}{\sigma}\left(\partial_t\,\nabla^2\Psi + \left\{\Psi\,,\nabla^2\Psi\right\}\right) &= R_T\,\partial_x\Psi - R_S\,\partial_x\Psi + \nabla^4\Psi && (1)\\
\partial_t\,T + \{\Psi\,,T\} &= \partial_x\Psi + \nabla^2 T && (2)\\
\partial_t\,S + \{\Psi\,,S\} &= \partial_x\Psi + \tau\nabla^2 S\,. && (3)
\end{aligned}$$

Here Ψ is the stream function, T is the temperature, and S is the salinity. Both T and S are deviations from linear profiles. The dimensionless constants used are the temperature and salt Rayleigh numbers

$$R_T = \frac{g\alpha\overline{T}_z d^4}{\nu\kappa_T},\qquad R_S = \frac{g\beta\overline{S}_z d^4}{\nu\kappa_T}, \tag{4}$$

and the Prandtl and Schmidt numbers

$$\sigma = \frac{\nu}{\kappa_T}, \qquad \tau = \frac{\kappa_S}{\kappa_T}, \tag{5}$$

where x is the horizontal direction, z the vertical, g is the acceleration due to gravity, α and β are the coefficients of thermal expansions for the heat and salt, $\overline{T}_z$ and $\overline{S}_z$ are the mean gradients of heat and salt, d is the vertical thickness of the fluid layer, ν is the viscosity of the fluid, κ_T and κ_S are the coefficients of heat and salt diffusion. The Jacobian is

$$\{F\,, G\} = \partial_x F\,\partial_z G - \partial_x G\,\partial_z F\,. \tag{6}$$

The problem was nondimensionalised so that $t \sim d^2/\kappa_T$, $x, z \sim d$, $T \sim \overline{T}_z d$, $S \sim \overline{S}_z d$. When surface tension effects are not present, for $R_T < 0$ and $R_S < 0$ the system is in the fingering regime, whereas for $R_T > 0$ and $R_S > 0$ the system is in the diffusive regime. The onset of instability for the fingering regime is direct, and for the diffusive case it is oscillatory (overstability) [5].

The difference between normal thermohaline convection and its Marangoni counterpart comes from the boundary conditions. We consider an infinite layer of fluid bounded above and below. At the bottom of the fluid there is a rigid plate with fixed flux boundary conditions on the heat and salt:

$$\Psi = \partial_z\Psi = \partial_z T = \partial_z S = 0, \quad z = 0, \tag{7}$$

whereas at the top there is a free surface having a surface tension with a linear temperature and salinity dependence

$$\sigma = \sigma_0 - \gamma_T(T - T_0) - \gamma_S(S - S_0), \tag{8}$$

so that there is a stress exerted at the top of the fluid [6, 7]. The boundary conditions at the top surface are thus

$$\begin{aligned} \Psi &= \partial_z T = \partial_z S = 0, \\ \nabla^2\Psi &= M_T\,\partial_x T + M_S\,\partial_x S, \qquad z = 1, \end{aligned} \tag{9}$$

where the temperature and salinity Marangoni numbers are defined as

$$M_T = \frac{\gamma_T\,\overline{T}_z d^2}{\rho\,\nu\kappa_T}, \quad M_S = \frac{\gamma_S\,\overline{S}_z d^2}{\rho\,\nu\kappa_T}\;, \tag{10}$$

and ρ is the density of the fluid. The quantities $\gamma_{T,S}$ can have either sign depending on the diffusing components, and in particular for the heat–salt system

$$\gamma_T = 0.157\ \mathrm{dyn\ cm^{-1}\,K^{-1}}, \quad \gamma_S = -0.367\ \mathrm{dyn\ cm^{-1}\,wt\%^{-1}}. \tag{11}$$

We neglect here possible deformation of the surface (for inclusion of this effect see [8, 9, 10, 11]). At lowest order there it is possible to use the *crispation* number to take surface deformation effects into account, which leads to a long wave instability. We also find such instabilities here, but as a result of the fixed heat and salt flux condition in Eqs. 7 and 9, which distinguishes this work from previous ones [6, 12].

3 Linear Stability

The system of equations 1–3 can be written with a linear and a nonlinear part

$$\mathcal{L}\,\mathbf{\Psi} = \mathcal{N}(\mathbf{\Psi}, \mathbf{\Psi}), \tag{12}$$

where the state vector is

$$\mathbf{\Psi} = \begin{pmatrix} \Psi \\ T \\ S \end{pmatrix}, \tag{13}$$

the linear operator is given by

$$\mathcal{L} = \begin{pmatrix} \nabla^4 - \frac{1}{\sigma}\partial_t \nabla^2 & R_T\,\partial_x & -R_S\,\partial_x \\ \partial_x & \nabla^2 - \partial_t & 0 \\ \partial_x & 0 & \tau\,\nabla^2 - \partial_t \end{pmatrix}, \tag{14}$$

and the nonlinear terms by

$$\mathcal{N}(\mathbf{\Psi}, \mathbf{\Psi}) = \begin{pmatrix} \{\Psi\,, \nabla^2\Psi\} \\ \{\Psi\,, T\} \\ \{\Psi\,, S\} \end{pmatrix}. \tag{15}$$

We now look at the linear problem. The nonlinear terms $\mathcal{N}$ drop out and we can focus our attention on only one Fourier mode in the x direction with wavenumber a, so we write

$$\mathbf{\Psi} = A\,e^{\mathrm{i}(ax \pm \omega t)} \begin{pmatrix} \psi_\pm(z) \\ -\mathrm{i}\,\Theta_\pm(z) \\ -\mathrm{i}\,\Sigma_\pm(z) \end{pmatrix} + \text{c.c.}\,, \tag{16}$$

where we separate the x and z dependence and in doing so define the complex functions ψ, Θ, and Σ. We have set the real part of the time dependence to zero to look for marginal modes. We then have to solve the linear set of equations

$$((D^2 - a^2) \mp \mathrm{i}\,\frac{\omega}{\sigma})(D^2 - a^2)\,\psi_\pm \;=\; -aR_T\,\Theta_\pm + aR_S\,\Sigma_\pm \tag{17}$$

$$((D^2 - a^2) \mp \mathrm{i}\,\omega)\,\Theta_\pm \;=\; a\,\psi_\pm \tag{18}$$

$$(\tau(D^2 - a^2) \mp \mathrm{i}\,\omega)\,\Sigma_\pm \;=\; a\,\psi_\pm\,. \tag{19}$$

We vary a and solve numerically for R_T and ω using a code written by N. Baker and D. Moore implementing the Newton–Raphson–Kantorovich method. The marginal stability curve and Hopf frequency plotted against a are shown in Figure 1 for the diffusive case ($R_T > 0$, $R_S > 0$). There is an instability at $a = 0$, corresponding to the diffusive instability. There is also another instability at nonzero a, a mode driven by surface tension. It can be seen from the figure that by varying parameters it is possible for these two instabilities to come in at the same critical Rayleigh number R_{Tc}.

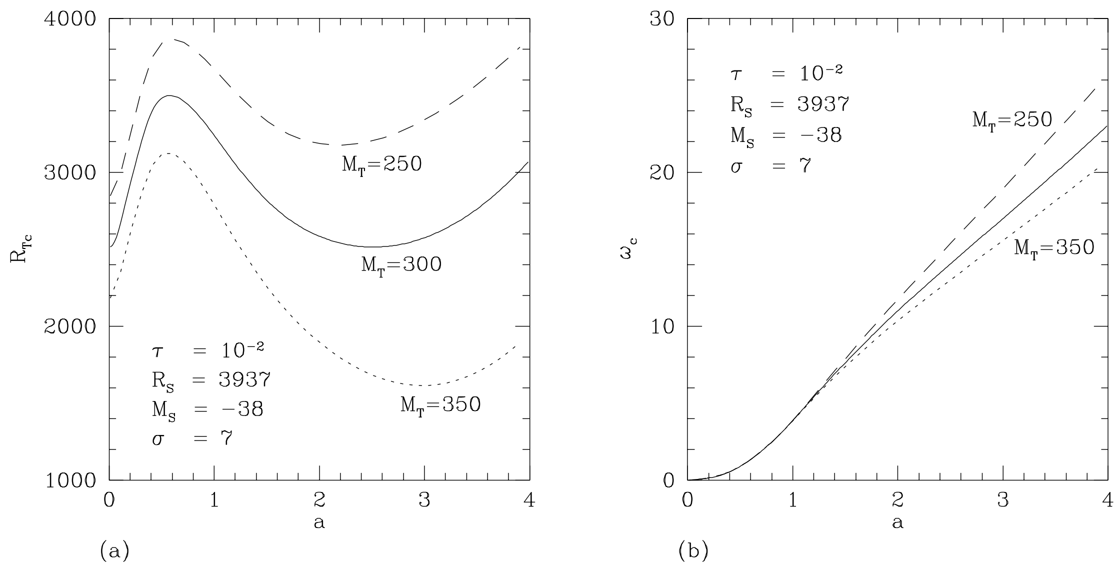

Figure 1: Marginal stability curve (a) and Hopf frequency (b) for the diffusive case. $M_T = 300$ represents the case for which both the $a = 0$ (double-diffusive) and nonzero a (surface tension) instabilities linearly come in together.

The density ratio R_ρ is defined to be the density gradient of the stabilizing component over the destabilizing one, which for the diffusive case is

$$R_\rho = \frac{\beta\,\overline{S}_z}{\alpha\,\overline{T}_z} = \frac{R_S}{R_T}. \tag{20}$$

All the curves in Figure 1 have $R_\rho > 1$ and correspond therefore to statically stable situations in the absence of surface tension.

4 Finite Wavenumber Instability

Figure 2 shows the eigenfunctions of the system for the solid line in Figure 1. Note the real part of the salinity eigenfunction has an extremum below $z = 1$. This may be due to the much lower diffusivity of salt.

Some idea of the development of the instability at finite wavenumber may be gained by the usual kind of weakly nonlinear theory. This must be done numerically, at least partly, for this instability and requires us to evaluate the adjoint to the linear system Eqs. 17–19. The equations of the adjoint problem for this system are straightforward to obtain. Specifically, one just takes the transpose of the matrix Eq. 14 and let $\partial_x \to -\partial_x$ and $\partial_t \to -\partial_t$. However, a complication arises because of the surface terms when one writes

$$\int_0^1 \mathbf{\Psi}^\dagger\,\mathcal{L}\,\mathbf{\Psi}\,dz = \text{surface terms} + \int_0^1 \mathcal{L}^\dagger\,\mathbf{\Psi}^\dagger\,\mathbf{\Psi}\,dz\,; \tag{21}$$

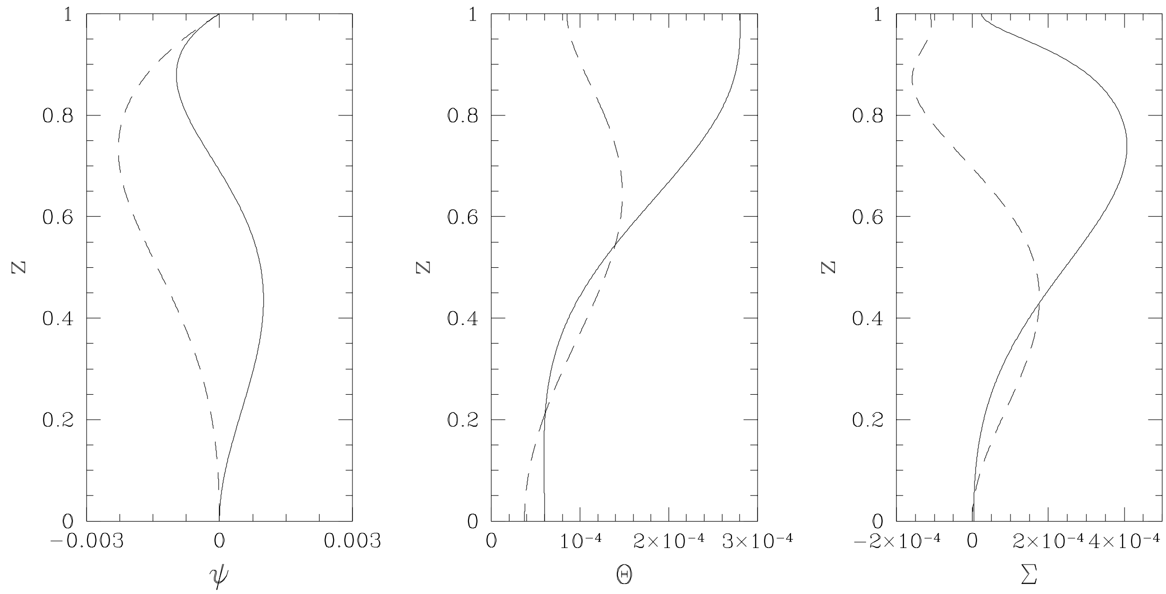

Figure 2: Linear eigenfunctions of ψ, Θ, and Σ at the $a = 2.5$ minimum of the solid curve ($M_T = 300$) in Figure 1. The solid line is the real part and the dashed line the imaginary part. The Hopf frequency is $\omega = 14.1$.

We will not show this in detail here, but in order for the surface terms to vanish, one must take for the boundary conditions on the adjoint

$$\mathbf{\Psi}^\dagger = D\,\mathbf{\Psi}^\dagger = D\,T^\dagger = D\,S^\dagger = 0, \qquad z = 0, \tag{22}$$

at the bottom surface and

$$\begin{aligned} \mathbf{\Psi}^\dagger &= 0, \\ D\,T^\dagger &= M_T\,\partial_x D\mathbf{\Psi}^\dagger, \\ D\,S^\dagger &= M_S\,\partial_x D\mathbf{\Psi}^\dagger, \qquad z = 1, \end{aligned}$$

at the top.

We can then use the solution to the adjoint problem to derive an amplitude equation for the nonzero a instability, calculating the coefficients numerically. This equation is valid for cases like the dotted curve ($M_T = 350$) in Figure 1, where the nonzero wavenumber instability occurs at a smaller thermal Rayleigh number. The amplitude equation obtained is, as expected, a complex Ginzburg–Landau equation:

$$\partial_T\,A = a_1\,A + a_2\,A_{XX} - a_3\,|A|^2 A\,. \tag{23}$$

The analysis of this equation, and its coupling with an equation for the long-wave instability, will be the topic of later work.

5 Long-Wave Expansion

We now focus our attention on the instability at $a = 0$ of the kind seen in Figure 1. We shall assume we are in a parameter range such that the marginal stability curve looks like the dashed line ($M_T = 250$) in Figure 1, so that the long wave mode goes unstable before the surface-tension driven instability at nonzero a. In the usual manner we assume that there is an expansion in a small parameter ε for the spatial and temporal dependence [13]

$$\begin{aligned} \partial_x &= \varepsilon^{1/2}\partial_X\,, \\ \partial_t &= \varepsilon\,\partial_{T_1} + \varepsilon^2\partial_{T_2}\,; \end{aligned} \tag{24}$$

The absence of a zeroth order x derivative reflects the fact that this instability occurs at $a = 0$. We define ϕ by

$$\psi(z) = \varepsilon^{1/2}\phi_X(z)\,, \tag{25}$$

so that all the equations contain only integer powers of ε. The remaining variables are also expanded in powers of ε, assuming their amplitudes are small:

$$\begin{aligned} \phi(X,z,T_1,T_2) &= \varepsilon\,\phi_1 + \varepsilon^2\,\phi_2 + \ldots \\ T(X,z,T_1,T_2) &= \varepsilon\,T_1 + \varepsilon^2\,T_2 + \ldots \\ S(X,z,T_1,T_2) &= \varepsilon\,S_1 + \varepsilon^2\,S_2 + \ldots\,, \end{aligned}$$

and the control parameters

$$\begin{aligned} R_T &= R_{T0} + \varepsilon\,R_{T1} + \varepsilon^2\,R_{T2} + \ldots \\ R_S &= R_{S0} + \varepsilon\,R_{S1} + \varepsilon^2\,R_{S2} + \ldots \\ M_T &= M_{T0} + \varepsilon\,M_{T1} + \varepsilon^2\,M_{T2} + \ldots \\ M_S &= M_{S0} + \varepsilon\,M_{S1} + \varepsilon^2\,M_{S2} + \ldots\,. \end{aligned}$$

We choose not to expand τ and σ. The operator $\mathcal{L}$ and the nonlinear terms $\mathcal{N}$ also have an expansion

$$\mathcal{L} = \mathcal{L}_0 + \varepsilon\,\mathcal{L}_1 + \varepsilon^2\mathcal{L}_2 + \ldots \tag{26}$$

$$\mathcal{N} = \varepsilon^2\mathcal{N}_2 + \varepsilon^3\mathcal{N}_3 + \ldots\,, \tag{27}$$

with

$$\mathcal{L}_0 = \begin{pmatrix} D^4\partial_X & R_{T0}\partial_X & -R_{S0}\partial_X \\ 0 & D^2 & 0 \\ 0 & 0 & D^2 \end{pmatrix},$$

$$\mathcal{L}_1 = \begin{pmatrix} 2D^2\partial_X^3 - \sigma^{-1}\partial_{T_1}D^2\partial_X & R_{T1}\partial_X & -R_{S1}\partial_X \\ \partial_X^2 & \partial_X^2 - \partial_{T_1} & 0 \\ \partial_X^2 & 0 & \tau\,\partial_X^2 - \partial_{T_1} \end{pmatrix},$$

$$\mathcal{L}_2 = \begin{pmatrix} \partial_X^5 - \sigma^{-1}(\partial_{T_2} D^2 \partial_X + \partial_{T_1}\partial_X^3) & R_{T2}\partial_X & -R_{S2}\partial_X \\ 0 & -\partial_{T_2} & 0 \\ 0 & 0 & -\partial_{T_2} \end{pmatrix},$$

$$\mathcal{N}_2 = \begin{pmatrix} \sigma^{-1}(\phi_{0XX} D^3\phi_{0X} - D\phi_{0X} D^2\phi_{0XX}) \\ \phi_{0XX} D\Theta_0 - D\phi_{0X}\Theta_{0X} \\ \phi_{0XX} D\Sigma_0 - D\phi_{0X}\Sigma_{0X} \end{pmatrix},$$

$$\mathcal{N}_3 = \begin{pmatrix} \sigma^{-1}(\phi_{0XX} D^3\phi_{1X} - D\phi_{0X} D^2\phi_{1XX} + \phi_{1XX} D^3\phi_{0X} - D\phi_{1X} D^2\phi_{0XX}) \\ \phi_{0XX} D\Theta_1 - D\phi_{0X}\Theta_{1X} + \phi_{1XX} D\Theta_0 - D\phi_{1X}\Theta_{0X} \\ \phi_{0XX} D\Sigma_1 - D\phi_{0X}\Sigma_{1X} + \phi_{1XX} D\Sigma_0 - D\phi_{1X}\Sigma_{0X} \end{pmatrix},$$

where we are using a slightly modified state vector with ϕ in the first slot instead of ψ:

$$\Phi(X, z, T_1, T_2) = \begin{pmatrix} \phi \\ \Theta \\ \Sigma \end{pmatrix}. \tag{28}$$

The boundary conditions at the bottom rigid surface are

$$\phi_X = D\,\phi_X = D\Theta = D\Sigma = 0, \quad z = 0; \tag{29}$$

and at the top surface

$$\begin{aligned} &\phi_X = D\Theta = D\Sigma = 0, \\ &D^2\phi_X = M_T\,\Theta_X + M_S\,\Sigma_X, \quad z = 1; \end{aligned} \tag{30}$$

where the last boundary condition is different at each order since there is an expansion for M_T and M_S.

For the case of fixed flux boundary conditions the solvability condition at each order is simply

$$\int_0^1 D^2\Theta\,dz = \int_0^1 \tau\,D^2\Sigma\;dz = 0. \tag{31}$$

We are now ready to proceed with the expansion.

5.1 Order ε^0

The zeroth order equations are simply $\mathcal{L}_0\,\Phi_0 = 0$:

$$\begin{aligned} D^4\phi_{0X} &= -R_{T0}\,\Theta_{0X} + R_{S0}\,\Sigma_{0X}, \\ D^2\Theta_0 &= 0, \\ \tau\,D^2\Sigma_0 &= 0. \end{aligned}$$

The Θ_0 and Σ_0 equations together with the boundary conditions tell us that these two quantities are independent of z. Hence we can integrate the first equation four times to obtain ϕ_{0X}, which after applying the boundary conditions becomes

$$\begin{aligned} \phi_{0X} &= \frac{z^2(z^2-1)}{48}\left[((3-2z)R_{T0} + 12M_{T0})\Theta_{0X} - ((3-2z)R_{S0} - 12M_{S0})\Sigma_{0X}\right], \\ &= -b_{T0}(z)\,\Theta_{0X} + b_{S0}(z)\,\Sigma_{0X}, \end{aligned} \tag{32}$$

which defines $b_{T0}(z)$ and $b_{S0}(z)$. The solvability condition is automatically satisfied at this order, since the right-hand-side of the temperature and salinity equations vanishes.

5.2 Order ε^1

The first order system is $\mathcal{L}_0\Phi_1 + \mathcal{L}_1\Phi_0 = 0$:

$$\begin{aligned}
D^4\phi_{1X} &= -R_{T1}\,\Theta_{0X} + R_{S1}\,\Sigma_{0X} - R_{T0}\,\Theta_{1X} + R_{S0}\,\Sigma_{1X} \\
&\quad - 2D^2\phi_{0XXX} + \sigma^{-1}\partial_{T_1} D^2\phi_{0X}\,, \\
D^2\Theta_1 &= -\phi_{0XX} - \Theta_{0XX} + \partial_{T_1}\Theta_0\,, \\
\tau\, D^2\Sigma_1 &= -\phi_{0XX} - \tau\,\Sigma_{0XX} + \partial_{T_1}\Sigma_0\,,
\end{aligned} \tag{33}$$

where we have used the fact that $D\Theta_0 = D\Sigma_0 = 0$. We integrate the Θ_1 and Σ_1 equations to get the solvability condition

$$\begin{aligned}
\left\langle D^2\Theta_1\right\rangle &= -\langle\phi_{0XX}\rangle - \Theta_{0XX} + \partial_{T_1}\Theta_0 = 0, \\
\left\langle \tau\, D^2\Sigma_1\right\rangle &= -\langle\phi_{0XX}\rangle - \tau\,\Sigma_{0XX} + \partial_{T_1}\Sigma_0 = 0,
\end{aligned} \tag{34}$$

where

$$\langle f\rangle \equiv \int_0^1 f\,dz\,. \tag{35}$$

Using the previous order result, we have

$$\begin{aligned}
\langle\phi_{0XX}\rangle &= \langle b_{S0}\rangle\,\Sigma_{0XX} - \langle b_{T0}\rangle\,\Theta_{0XX}\,, \\
&= \left(\frac{R_{S0}}{320} - \frac{M_{S0}}{48}\right)\Sigma_{0XX} - \left(\frac{R_{T0}}{320} + \frac{M_{T0}}{48}\right)\Theta_{0XX}\,.
\end{aligned} \tag{36}$$

Then we can rewrite Eq. 34 as

$$\partial_{T_1}\begin{pmatrix}\Theta_0\\ \Sigma_0\end{pmatrix} = M\begin{pmatrix}\Theta_{0XX}\\ \Sigma_{0XX}\end{pmatrix} \tag{37}$$

where

$$M = \begin{pmatrix} 1 - \langle b_{T0}\rangle & \langle b_{S0}\rangle \\ -\langle b_{T0}\rangle & \tau + \langle b_{S0}\rangle \end{pmatrix}\,. \tag{38}$$

Now assume M has a complex eigenvalues $\lambda_\pm$. Then the solution to Eq. 37 is that the linear combinations of Θ_0 and Σ_0 along the eigenvectors of M (call them $\widetilde{\Theta}_\pm$) evolve as

$$\widetilde{\Theta}_\pm(X,T_1,T_2) = e^{\alpha\,X + \lambda_\pm\,\alpha^2 T_1}\,\widehat{\Theta}_\pm(T_2)\,, \tag{39}$$

where α is a constant. We require that the real part of $\lambda_\pm$ vanish to avoid exponentially growing or decaying solutions at this order. If we assume that the $\lambda_\pm$ are real and that only λ_+ vanishes, then we have a steady bifurcation; continuing with the long-wave expansion then leads to an equation as in [14]. If the imaginary part of $\lambda_\pm$ does not vanish, we get a diffusive-type linear O.D.E., thereby fixing the X dependence of Θ_0 and Σ_0. Thus we need to introduce another, longer length scale in order to get a partial differential equation and in the end we get a complex Ginzburg–Landau equation. This calculation simply amounts to rescaling the problem and doing an expansion like that in Section 4. Both the oscillatory and steady instabilities can be captured in a single long-wave equation if we can tune the system such that both the eigenvalues of M vanish in real and imaginary part. This specially tuned system corresponds to the Takens–Bogdanov bifurcation point, where branches of oscillatory and steady instabilities meet [15].

The tuning is achieved by imposing that M have zero eigenvalues, i.e. that its determinant and trace vanish:

$$\tau\,(1-\langle b_{T0}\rangle)+\langle b_{S0}\rangle=0, \qquad \langle b_{S0}\rangle-\langle b_{T0}\rangle+\tau+1=0\,. \tag{40}$$

The values of $\langle b_{T0}\rangle$ and $\langle b_{S0}\rangle$ at this point are

$$\langle b_{T0}\rangle=\frac{1}{1-\tau}\,, \qquad \langle b_{S0}\rangle=\frac{\tau^2}{1-\tau}\,, \tag{41}$$

and the matrix M simplifies to

$$M=\frac{\tau}{\tau-1}\begin{pmatrix}1 & -\tau\\ \tau^{-1} & -1\end{pmatrix}\,. \tag{42}$$

In terms of the physical parameters, we have

$$\begin{aligned} R_{T0} &= \frac{320}{1-\tau}-\frac{20}{3}M_{T0}\,,\\ R_{S0} &= \frac{320\,\tau^2}{1-\tau}+\frac{20}{3}M_{S0}\,; \end{aligned}$$

that is, the co-dimension two tuning of R_T and R_S at the Takens–Bogdanov point. The matrix M has only one eigenvector, $\mathbf{e}_1=(\tau\ 1)$. Any other vector is projected onto $\mathbf{e}_1$ by M. We could make a coordinate transformation to put M in Jordan form

$$\widetilde{M}=\begin{pmatrix}0 & 1\\ 0 & 0\end{pmatrix}\,, \tag{43}$$

but we will not find it necessary to do so here.

Thus we have

$$\Theta_0=\tau\,\Sigma_0\,, \tag{44}$$

and the solvability condition, Eq. 37, is now just

$$\partial_{T_1}\begin{pmatrix}\Theta_0\\ \Sigma_0\end{pmatrix}=0. \tag{45}$$

It now remains for us to solve the system of equations given by 33. We can rewrite the solution for ϕ_{0X} as

$$\phi_{0X} = P_1(z)\,\Theta_{0X}\,, \tag{46}$$

where

$$P_1(z) = \frac{z^2(z-1)}{48}\left[(3-2z)\left(R_{T0} - \frac{R_{S0}}{\tau}\right) + 12\left(M_{T0} + \frac{M_{S0}}{\tau}\right)\right]. \tag{47}$$

Integrating the temperature and salinity equations twice and applying the fixed flux boundary conditions we find

$$\begin{aligned}
\Theta_1 &= \left(\frac{z^2}{2} - P_1^{(-2)}(z)\right)\Theta_{0XX} + \Theta_{1,0}\,,\\
\tau\,\Sigma_1 &= \left(\frac{z^2}{2} - P_1^{(-2)}(z)\right)\Theta_{0XX} + \tau\,\Sigma_{1,0}\,,\\
&= \Theta_1 - \Theta_{1,0} + \tau\,\Sigma_{1,0}\,,
\end{aligned} \tag{48}$$

where the notation $P_1^{(n)}(z)$ means that P_1 is differentiated n times, or integrated for $n < 0$. The z-independent quantities $\Theta_{1,0}$ and $\Sigma_{1,0}$ are integration constants that can depend on X and T_2. The equation for ϕ_{1X} is

$$\begin{aligned}
D^4\phi_{1X} &= -R_{T0}\Theta_{1,0X} + R_{S0}\Sigma_{1,0X} + \left(\frac{R_{S1}}{\tau} - R_{T1}\right)\Theta_{0X}\\
&\quad + \left[\left(\frac{R_{S0}}{\tau} - R_{T0}\right)\left(\frac{z^2}{2} - P_1^{(-2)}(z)\right) - 2P_1^{(2)}(z)\right]\Theta_{0XXX}\,.
\end{aligned} \tag{49}$$

We wish to integrate this four times and apply the boundary conditions. The calculation will not be shown in detail here. Instead, we write

$$\phi_{1X} = -b_{T0}(z)\,\Theta_{1,0X} + b_{S0}(z)\,\Sigma_{1,0X} + P_2(z)\,\Theta_{0X} + P_3(z)\,\Theta_{0XXX}\,. \tag{50}$$

5.3 Order ε^2

At this order we have $\mathcal{L}_0\Phi_2 + \mathcal{L}_1\Phi_1 + \mathcal{L}_2\Phi_0 = \mathcal{N}_2$:

$$\begin{aligned}
D^4\phi_{2X} &= -R_{T0}\,\Theta_{2X} + R_{S0}\,\Sigma_{2X} - R_{T1}\,\Theta_{1X} + R_{S1}\,\Sigma_{1X}\\
&\quad - R_{T2}\,\Theta_{0X} + R_{S2}\,\Sigma_{0X} - 2D^2\phi_{1XXX} - \phi_{0XXXXX} + \sigma^{-1}\partial_{T_2}D^2\phi_{0X}\\
&\quad + \sigma^{-1}(\phi_{0XX}D^3\phi_{0X} - D\phi_{0X}D^2\phi_{0XX})\,,\\
D^2\Theta_2 &= -\phi_{1XX} - \Theta_{1XX} + \partial_{T_2}\Theta_0 - D\phi_{0X}\Theta_{0X}\,,\\
\tau\,D^2\Sigma_2 &= -\phi_{1XX} - \tau\,\Sigma_{1XX} + \partial_{T_2}\Sigma_0 - D\phi_{0X}\Sigma_{0X}\,.
\end{aligned} \tag{51}$$

We integrate the heat and salt equations in the usual manner to get the solvability conditions

$$\begin{aligned}
\Theta_{0\,T_2} &= \langle\phi_{1XX}\rangle + \langle\Theta_{1XX}\rangle\,,\\
\Sigma_{0\,T_2} &= \langle\phi_{1XX}\rangle + \langle\tau\,\Sigma_{1XX}\rangle\,,
\end{aligned} \tag{52}$$

where the nonlinear terms dropped out because of the boundary conditions. We can rewrite this as

$$\left(\begin{array}{c}\Theta_{0T_2}\\ \Sigma_{0T_2}\end{array}\right) = M\left(\begin{array}{c}\Theta_{1,0XX}\\ \Sigma_{1,0XX}\end{array}\right) + \langle P_2\rangle \left(\begin{array}{c}\Theta_{0XX}\\ \Sigma_{0XX}\end{array}\right) + \left\langle P_3 - P_1^{(-2)} + \frac{z^2}{2}\right\rangle \left(\begin{array}{c}\Theta_{0XXXX}\\ \Sigma_{0XXXX}\end{array}\right). \tag{53}$$

We define χ by

$$\begin{aligned}\left(\begin{array}{c}\Theta_{1,0}\\ \Sigma_{1,0}\end{array}\right) &= \Sigma_{1,0}\left(\begin{array}{c}\tau\\ 1\end{array}\right) + \frac{\tau-1}{\tau}\left(\begin{array}{c}\chi\\ 0\end{array}\right),\\ &= \Sigma_{1,0}\,\mathbf{e}_1 + \frac{\tau-1}{\tau}\,\chi\,\mathbf{e}_2\,,\end{aligned}$$

or

$$\chi = \frac{\tau}{\tau-1}\left(\Theta_{1,0} - \tau\,\Sigma_{1,0}\right)\,. \tag{54}$$

These conditions on the parameters amount to tuning the Takens–Bogdanov point at order ε^2. The solvability condition Eq. 53 can be written

$$\left(\begin{array}{c}\Theta_{0T_2}\\ \Theta_{0T_2}/\tau\end{array}\right) = \left(\begin{array}{c}\chi_{XX}\\ \chi_{XX}/\tau\end{array}\right) + \langle P_2\rangle \left(\begin{array}{c}\Theta_{0XX}\\ \Sigma_{0XX}\end{array}\right) + \left\langle P_3 - P_1^{(-2)} + \frac{z^2}{2}\right\rangle \left(\begin{array}{c}\Theta_{0XXXX}\\ \Sigma_{0XXXX}\end{array}\right). \tag{55}$$

These two equations can only be consistent for $\tau \neq 1$ if

$$\langle P_2\rangle = \left\langle P_3 - P_1^{(-2)} + \frac{z^2}{2}\right\rangle = 0, \tag{56}$$

which means, after integrating the polynomials,

$$\begin{aligned}\frac{R_{S2}}{\tau} - R_{T2} &= \frac{20}{3}\left(M_{T2} + \frac{M_{S2}}{\tau}\right)\\ M_{T0} + \frac{M_{S0}}{\tau} &= 48\frac{(32 \pm \sqrt{210194})}{241}.\end{aligned} \tag{57}$$

Then the solvability condition at this order is

$$\Theta_{0T_2} = \chi_{XX}\,. \tag{58}$$

5.4 Order ε^3

Avoiding detailed calculations, we simply quote the result for the solvability condition at this order[1]

$$\chi_{T_2} = -\nu\,\chi_{XX} + \mu\,\Theta_{0XXXX} + \lambda\,\Theta_{0XX} - \rho\,\chi_{XXXX} - \gamma\,\Theta_{0XXXXXX} + \zeta\,(\Theta_{0X}^2)_{XX}\,, \tag{59}$$

[1]This calculation was done on Wolfram Research's *Mathematica* software package.

where

$$
\begin{aligned}
\nu &= \frac{(1-\tau)}{960}\,(3\,R_{T2}+20\,M_{T2})\,,\\
\mu &= \sqrt{\frac{9577}{22}}\,\frac{(R_{T2}\,\tau - R_{S2})}{75600}\,,\\
\lambda &= \frac{M_{T4}\,\tau + M_{S4}}{48}\,,\\
\rho &= \frac{142}{1687}+\frac{5\sqrt{\frac{9577}{22}}}{15183}-\frac{M_{T0}}{90720}-\frac{\sqrt{\frac{9577}{22}}\,M_{T0}}{22680}+\frac{M_{T0}\,\tau}{90720}\\
&\qquad +\frac{\sqrt{\frac{9577}{22}}\,M_{T0}\,\tau}{22680}+\frac{1213\,\tau}{25305\,\sigma}+\frac{\sqrt{\frac{105347}{2}}\,\tau}{50610\,\sigma}\,,\\
\gamma &= \frac{\left(144945779034529+64636181572\,\sqrt{210694}\right)}{10129277026793925}\,\tau\,,\\
\zeta &= \frac{-1}{439092360\,\sigma}(523104000\,\sigma+3766800\,\sqrt{210694}\,\sigma-18603995\,M_{T0}\,\sigma\\
&\quad -9640\,\sqrt{210694}\,M_{T0}\,\sigma+293982984\,\tau+887832\,\sqrt{210694}\,\tau\\
&\quad +18603995\,M_{T0}\,\sigma\,\tau+9640\,\sqrt{210694}\,M_{T0}\,\sigma\,\tau)\,.
\end{aligned}
$$

We have eliminated M_{S0} from these coefficients by taking the positive solution of Eq. 57 for definiteness.

6 Analysis of the System

From now on we write T for T_2 and drop the subscript 0 on Θ_0. The system of long wave equations describing the small amplitude behaviour is thus

$$
\begin{aligned}
\Theta_T &= \chi_{XX}\,,\\
\chi_T &= -\nu\,\chi_{XX}+\mu\,\Theta_{XXXX}+\lambda\,\Theta_{XX}-\rho\,\chi_{XXXX}-\gamma\,\Theta_{XXXXXX}+\zeta\,(\Theta_X^2)_{XX}.
\end{aligned}
$$

This can be written as a partial differential equation, second order in time:

$$
\begin{aligned}
\Theta_{TT} &= -\nu\,\Theta_{XXT}-\rho\,\Theta_{XXXXT}+\mu\,\Theta_{(6X)}+\lambda\,\Theta_{XXXX}\\
&\quad -\gamma\,\Theta_{(8X)}+\zeta\,(\Theta_X^2)_{XXXX}.
\end{aligned}
\tag{60}
$$

We now make a spectral expansion of the system.

6.1 Galerkin Truncation

We use a truncated expansion for Θ:

$$
\Theta = A\,e^{\mathrm{i}KX}+B\,e^{2\,\mathrm{i}KX}+\text{c.c.},
\tag{61}
$$

neglecting higher harmonics. Then by using Eq. 60 we obtain a set of coupled O.D.E.'s for A and B:

$$\begin{aligned}
\ddot{A} &= K^2(\nu - \rho K^2)\dot{A} + K^4(\lambda - \mu K^2 - \gamma K^4)A + 4\,\zeta K^6 A^* B, \\
\ddot{B} &= 4K^2(\nu - 4\rho K^2)\dot{B} + 16K^4(\lambda - 4\mu K^2 - 16\gamma K^4)B - 16\,\zeta K^6 A^2.
\end{aligned} \tag{62}$$

Let

$$\begin{aligned}
\alpha(K) &= \lambda - \mu K^2 - \gamma K^4, \\
\beta(K) &= \nu - \rho K^2\,,
\end{aligned} \tag{63}$$

and abbreviate $\alpha(K)$ by α_1 and $\alpha(2\,K)$ by α_2 (similarly for β_1 and β_2). The linear dispersion relation for mode j is

$$\Gamma_j^2 - K_j^2 \beta_j\,\Gamma_j - K_j^4 \alpha_j = 0. \tag{64}$$

For a direct mode slightly above criticality we have $\Gamma_j = \epsilon \ll 1$, so that

$$\Gamma_j = \epsilon = -K_j^2 \frac{\alpha_j}{\beta_j}\,.$$

For a Hopf mode slightly above criticality, we have $\Gamma_j = \epsilon + \mathrm{i}\,\omega$ and

$$\epsilon = K_j^2\,\frac{\beta_j}{2}, \qquad \omega^2 = -K_j^4\left(\frac{\beta_j^2}{4} + \alpha_j\right).$$

6.2 Low-order Bifurcation Structure

We first look for steady nonlinear solutions of Eqs. 62. Assume $\dot{A} = \dot{B} = 0$. Then we can solve for the amplitude of A:

$$|A|^2 = -\frac{\alpha_1\,\alpha_2}{4\,K^4\,\zeta^2}\,. \tag{65}$$

We see that the mode will be supercritical if α_1 and α_2 have opposite signs, and subcritical if they have the same sign. The sign of ζ is immaterial. This first case is illustrated in Figure 3. The solid line corresponds to the $K = 1$ mode and the dashed line is the $K = 2$ mode, which is unstable. The second case is seen in Figure 4(a). The B mode (solid line) now becomes unstable before the subcritical A mode (dashed line). Figure 4(b) shows a plot of Θ as a function of X for different values of λ along the subcritical dashed line of (a). It can be seen from this figure that this is a mixed mode, and the mode develops a higher harmonic as the unsteady branch nears the steady B branch.

For a Hopf mode the amplitude and frequency are

$$\begin{aligned}
|A|^2 &= \frac{4\,K^4\omega^2\beta_1\,\beta_2 - (\omega^2 + K^4\alpha_1)(\omega^2 + 16K^4\alpha_2)}{64\,K^{12}\,\zeta^2}, \\
\omega^2 &= -4\,K^4\,\frac{\alpha_1\,\beta_2 + 4\,\alpha_2\,\beta_1}{\beta_1 + 4\,\beta_2}.
\end{aligned}$$

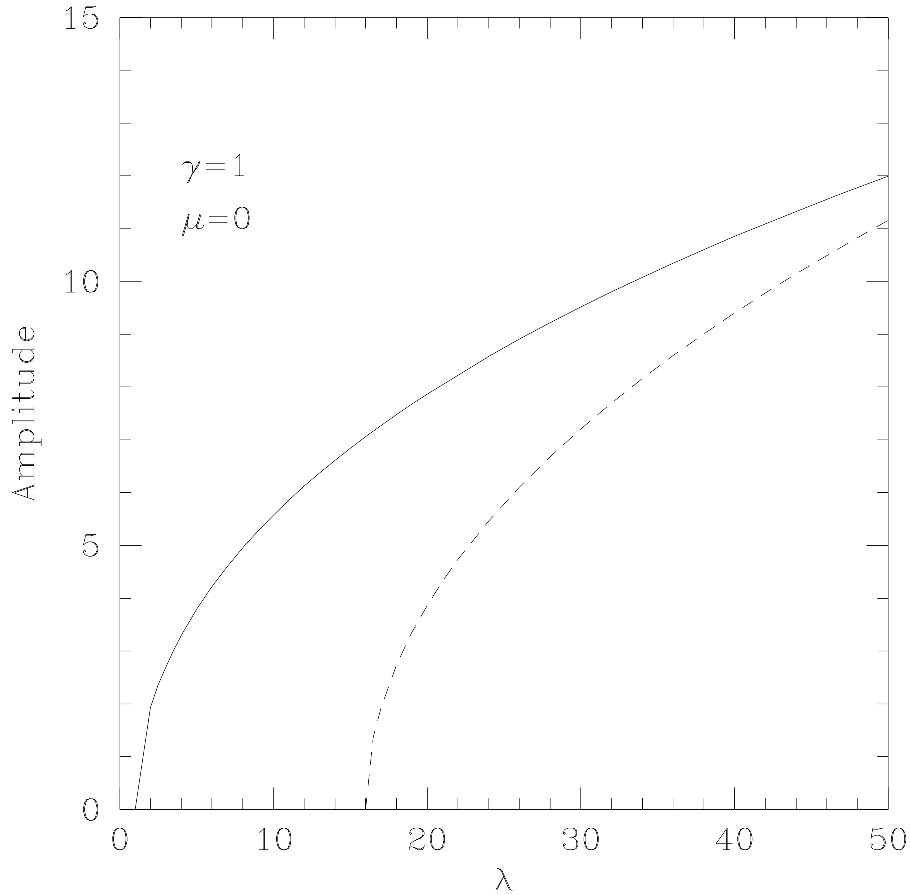

Figure 3: Summed amplitude of Fourier modes of a Galerkin truncation containing 20 modes, for the case in which A is supercritical and B is unstable. The dynamics of the system are very well approximated by the two-mode truncation.

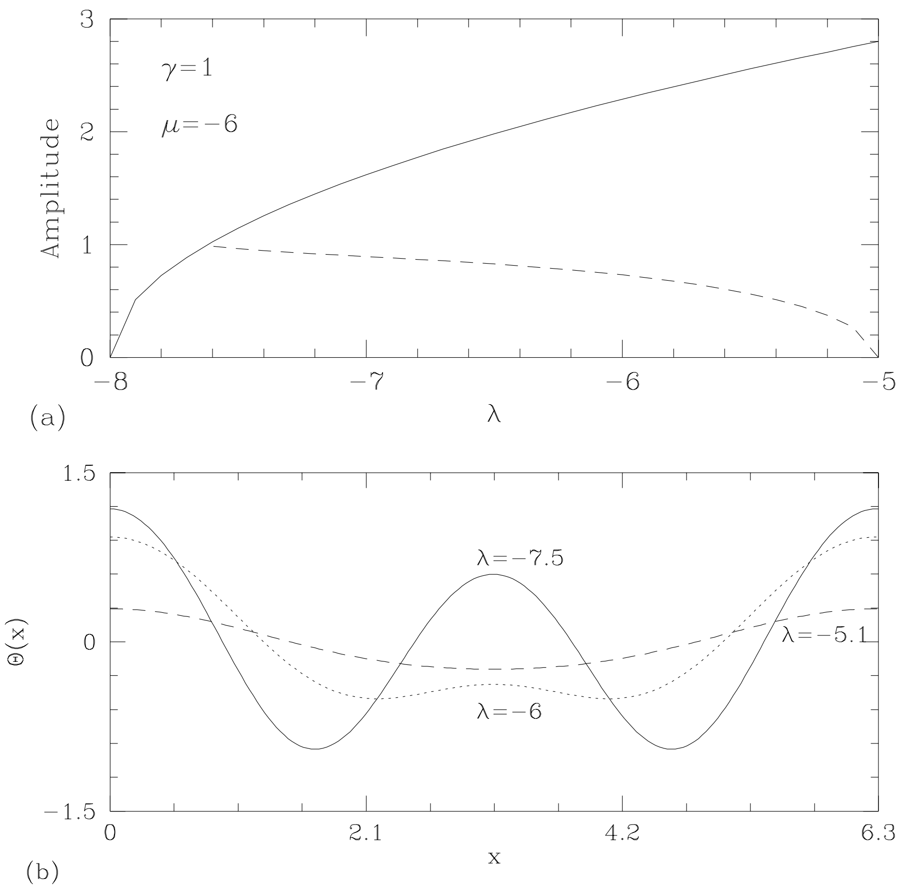

Figure 4: (a) Summed amplitude of Fourier modes of a Galerkin truncation containing 30 modes, for the case in which the B mode (solid line) becomes unstable before the subcritical A mode (dashed line). The two mode truncation approximates the dynamics very well. (b) Plot of Θ as a function of X for different values of λ along the subcritical dashed line of (a). It can be seen from this that the mode develops a higher harmonic as the unsteady branch nears the steady B branch, and is a pure $2K$ mode when they meet.

The Hopf branch is supercritical if

$$\frac{(\alpha_1 - 16\,K^4\alpha_2)^2}{4\,K^2\beta_2} > K^2\,\alpha_1\,\beta_2\,. \tag{66}$$

Now if the B mode is damped when the Hopf bifurcation for the A mode occurs ($\alpha_1 < 0$ for Hopf), we will have a subcritical bifurcation. The question is now whether this Hopf branch turns around at the next order ($|A|^4 A$). We have not yet worked this out, though the author and Neil J. Balmforth have a wager on the matter. If the branch does not turn around it will point to the fact that the expansion only captures the lowest order Takens–Bogdanov bifurcation structure, a result which is expected. [16]

After including a $C\,\exp(3\,\mathrm{i}\,KX)$ term in the Galerkin expansion we find the amplitude of the Hopf mode to order $|A|^4 A$ satisfies (letting $K=1$)

$$\begin{aligned} A \;=\; & -\frac{64\,\zeta^2\,|A|^2\,A}{(\alpha_1 + \mathrm{i}\,\beta_1\,\omega + \omega^2)(\alpha_2 + 4\,\mathrm{i}\,\beta_2\,\omega + 16\,\omega^2)} \\ & + \frac{48\cdot 16^2\cdot 81\,\zeta^4\,|A|^4\,A}{(\alpha_1 + \mathrm{i}\,\beta_1\,\omega + \omega^2)(\alpha_2 + 4\,\mathrm{i}\,\beta_2\,\omega + 16\,\omega^2)^2(\alpha_3 + 9\,\mathrm{i}\,\beta_3\,\omega + 81\,\omega^2)}. \end{aligned} \tag{67}$$

The problem is that in this system there is no way to tune out the $|A|^2 A$ term without also getting rid of the quintic nonlinearity. Hence the above equation is quite difficult to solve for A and ω.

7 Conclusions

We have a derived a small amplitude long wave equation for the double-diffusive Marangoni convection system. The expansion contains only a quadratic nonlinearity, of a different nature than that derived by Depassier and Spiegel [17] because of the additional X derivative: they had a nonlinearity of the form $(f^2)_{xx}$, whereas we have $(f_x^2)_{xx}$. The nonlinear term thus has the opposite effect (stabilizing for steady bifurcations) on the criticality of the system, as in [14].

We chose a small amplitude expansion because the physical system we studied does not contain enough parameters to tune out the resonant nonlinearities that arise in the order ε^2 solvability condition, Eq. 55, when the physical variables are of order one. However, including surface displacement effects (to lowest order, crispation [6, 12]) should allow us to do so and capture the full bifurcation structure of the Takens–Bogdanov point. We expect a system of the form

$$\begin{aligned} \Theta_T &= \chi_{XX}\,, \\ \chi_T &= -\nu\,\chi_{XX} + \mu\,\Theta_{XXXX} + \lambda\,\Theta_{XX} - \rho\,\chi_{XXXX} - \gamma\,\Theta_{XXXXXX} + q_1(\Theta_X^2)_{XXXX} \\ &\quad + q_2(\Theta_{XX}^2)_{XX} + q_3(\Theta_X^2)_{XX} + q_4(\Theta_X^3)_{XXX} + q_5(\Theta_X^4)_{XX} \\ &\quad + q_6(\chi\,\Theta_{XX})_{XX} + q_7(\chi_X\,\Theta_X)_{XX} + q_8(\chi_X\,\Theta_{XX})_X \end{aligned}$$

The equation has all the terms allowed by symmetry. If the system had an additional, up-down symmetry, only one nonlinearity with coefficient (q_4) would survive. Hence the equations above are potentially much richer than the Boussinesq up-down symmetric case. We can also use planform equations like the above to look for steady nonlinear solutions of the system [14].

Another direction to explore is the interaction of the $a = 0$ mode with the nonzero a mode when they occur together, as shown by the solid line in Figure 1. There will be a complex Ginzburg–Landau equation like Eq. 23 for the nonzero a mode and an equation of the type derived here for the $a = 0$ mode, with a coupling between them which should lead to interesting dynamics (see [8, 11] for theory and [9, 10] for experiments concerning the steady case, Marangoni single-diffusion). Another possible system for the study of this sort of long and finite length scale interaction is the case of compressible convection [13].

Acknowledgments

I am especially thankful to Neil Balmforth for being a great and available project supervisor, and for teaching me weakly nonlinear theory together with Keith Julien. I'm also indebted to nearly all the staff of the G.F.D. program, but I'd like to mention conversations with Lou Howard, Joe Keller, Oliver Kerr, Edgar Knobloch, Melvin Stern, Barry Ruddick, Edward Spiegel, Stewart Turner, and George Veronis. If I haven't learned double-diffusion properly from these people, I never will. Finally, I am grateful to all the other Fellows, for being a good laugh.

References

[1] C. F. Chen and T. F. Su, "Effect of surface tension on the onset of convection in a double-diffusive layer," Physics of Fluids A **4**, 2360 (1992).

[2] J. Tanny, C. C. Chen, and C. F. Chen, "Effects of interaction between Marangoni and double-diffusive instabilities," Journal of Fluid Mechanics **393**, 1 (1995).

[3] H. Bénard, "Les tourbillons cellulaires dans une nappe liquide," Revue générale des Sciences pures et appliquées **11**, 1261 (1900).

[4] J. R. A. Pearson, "On convection cells induced by surface tension," Journal of Fluid Mechanics **4**, 489 (1958).

[5] J. S. Turner, *Buoyancy Effects in Fluids* (Cambridge University Press, Cambridge, 1973).

[6] R. W. Zeren and W. C. Reynolds, "Thermal instabilities in two-fluid horizontal layers," Journal of Fluid Mechanics **53**, 305 (1972).

[7] D. A. Nield, “Onset of convection in a fluid layer overlying a layer of a porous medium,” Journal of Fluid Mechanics **81**, 513 (1977).

[8] A. A. Golovin, A. A. Nepomnyashchy, and L. M. Pismen, “Interaction bewteen short-scale Marangoni convection and long-scale deformational instability,” Physics of Fluids **6**, 34 (1994).

[9] M. F. Schatz, S. J. VanHook, W. D. McCormick, J. B. Swift, and H. L. Swinney, “Onset of surface-tension-driven Bénard convection,” Physical Review Letters **75**, 1938 (1995).

[10] S. J. VanHook, M. F. Schatz, W. D. McCormick, J. B. Swift, and H. L. Swinney, “Long-wavelength instability in surface-tension-driven Bénard convection,” Physical Review Letters **75**, 4397 (1995).

[11] A. A. Golovin, A. A. Nepomnyashchy, L. M. Pismen, and H. Riecke, “Steady and oscillatory side-band instabilities in Marangoni convection with deformable interface,” Preprint (1996).

[12] C. Pérez-García, “Linear stability analysis of Bénard–Marangoni convection in fluids with a deformable free surface,” Physics of Fluids A **3**, 292 (1991).

[13] M. C. Depassier and E. A. Spiegel, “The large-scale structure of compressible convection,” Astronomical Journal **86**, 496 (1981).

[14] C. J. Chapman and M. R. E. Proctor, “Nonlinear Rayleigh–Bénard convection between poorly conducting boundaries,” Journal of Fluid Mechanics **101**, 759 (1980).

[15] P. H. Coullet and E. A. Spiegel, “Amplitude equations for systems with competing instabilities,” SIAM Journal on Applied Mathematics **43**, 776 (1983).

[16] E. A. Spiegel, in *Proceedings of the 1981 Summer Program in Geophysical Fluid Dynamics*, Woods Hole, MA (Woods Hole Oceanographic Institute, Woods Hole, MA, 1981), p. 43.

[17] M. C. Depassier and E. A. Spiegel, “Convection with heat flux prescribed on the boundaries of the system. I. The effect of temperature dependence of material properties,” Geophysical and Astrophysical Fluid Dynamics **21**, 167 (1982).